

Application of a Fracture-Mechanics Approach to Gas Pipelines

Lubomír Gajdoš and Martin Šperl

Abstract—This study offers a new simple method for assessing an axial part-through crack in a pipe wall. The method utilizes simple approximate expressions for determining the fracture parameters K , J , and employs these parameters to determine critical dimensions of a crack on the basis of equality between the J -integral and the J -based fracture toughness of the pipe steel. The crack tip constraint is taken into account by the so-called plastic constraint factor C , by which the uniaxial yield stress in the J -integral equation is multiplied. The results of the prediction of the fracture condition are verified by burst tests on test pipes.

Keywords—Axial crack, Fracture-mechanics, J integral, Pipeline wall.

I. INTRODUCTION

IN thin-walled gas pipelines, similarly as in other (especially welded) structures, we should expect defects to occur. Under certain conditions, the defects can grow and they will gradually shorten the residual life of gas pipelines. Using fracture mechanics we can assess the threat that such defects can pose to the pipeline wall [1], [2], taking into account whether a brittle, quasi-brittle or ductile material is involved. A model description of crack-containing systems, based on the stress intensity factor (SIF), K , [3], [4] can be used for brittle and quasi-brittle fracture, and in addition for subcritical fatigue growth, corrosion fatigue and stress corrosion. In these cases, the surface crack is usually located in the field of one of the membrane tensile stress components or in the field of bending stress, or in a combination of these two stresses [5], [6]. The extent of the plastic zone at the crack tip is small in comparison with the dimensions of the crack and the cross section of the pipeline.

If the gas pipeline is made of a high toughness material, the plastic strains become extensive before the crack reaches instability. Hence, some elasto-plastic fracture mechanics methods, such as J -integral, crack opening displacement, the two-criterion method or some other procedure, should be employed to assess the fracture condition of the pipeline [7], [8].

The results of fracture tests on test pipes are invaluable when assessing the structural integrity of pressure pipelines.

L. GAJDOŠ, Senior Scientist, and M. ŠPERL, Postdoctoral Fellow, are with the Institute of Theoretical and Applied Mechanics – Academy of Sciences of the Czech Republic, v.v.i., Department of Thin-walled Structures, Prosecka 25, Prague 9, 190 00, Czech Republic. Contact e-mail: gajdos@itam.cas.cz, phone: 00420286882121.

Fracture tests not only provide particular experimental proof of the residual strength of pipelines containing cracks in the pipeline wall, which are the most dangerous type of defects. They also enable us to confront fracture theories directly with reality [9]. An evaluation of these fracture test results should always lead to information on whether a prediction of the fracture condition based on fracture criteria provides conservative, i.e. safe, fracture parameter values, and whether the degree of conservativeness of the prediction is not excessively high [10].

In this study a fracture-mechanics approach is used to predict the fracture condition of linepipe steel pipes. The approach utilizes simple approximate expressions for determining fracture parameters K , J , concerning the axial part-through thickness cracks in a pipe wall, and it employs these parameters to determine the critical dimensions of a crack on the basis of equality between the J integral and the J -based fracture toughness of the pipe steel. The crack tip constraint is accounted here by the so-called plastic constraint factor C , by which the uniaxial yield stress in the equation for determining the J integral is multiplied. The results of the prediction of the fracture condition of the pipes are verified by burst tests on test pipes.

II. A BRIEF BACKGROUND OF SOME FRACTURE – MECHANICS FORMULAE

A. SIF for an axial through crack

The stress intensity factor can be determined by (1)

$$K_I = M_T \sigma_\phi \sqrt{\pi c} \quad (1)$$

where:

$\sigma_\phi = pD/2t$ is the hoop stress, and

M_T is the Folias correction factor, taking account of curvature of a pipe.

Several expressions for determining the Folias factor can be found in various papers and compendia (e.g. [11], [12], [13]). One of the most widely used expressions is the following [14]:

$$M_T = \sqrt{1 + 1.255 \frac{c^2}{Rt} - 0.0135 \frac{c^4}{R^2 t^2}} \quad (2)$$

where:

R is the mean radius of the pipe, and
 t is the pipe wall thickness.

B. SIF for an axial part-through crack

Various methods are used for analyzing the problem of axial semi-elliptical surface cracks in the wall of a cylindrical shell (Fig. 1).

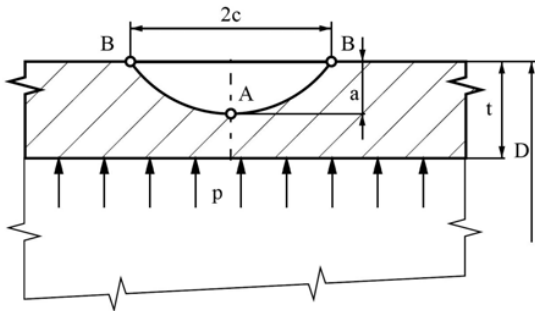


Fig. 1 An external longitudinal semi-elliptical crack in the wall of a cylindrical shell

A very good estimate of the stress intensity factor for such a crack is given by (3).

$$K_I = \left[M_F + \left(E(k) \sqrt{c/a} - M_F \right) \left(\frac{a}{t} \right)^p \right] \frac{\sigma_\phi \sqrt{\pi a}}{E(k)} M_{TM} \quad (3)$$

This is an adjusted form of the Newman solution [15] for a thin-walled shell. Here

M_F - a function depending on the crack geometry (on the ratio a/c),

$$E_k = \int_0^{\pi/2} \sqrt{1 - \frac{c^2 - a^2}{c^2} \sin^2 \theta} d\theta - \text{an elliptical integral of}$$

the second kind.

p - the function depending on the crack geometry (on the ratio a/c) and on the relative crack depth (on the ratio a/t)

$$M_{TM} = \frac{\left(1 - \frac{a/t}{M_T} \right)}{1 - a/t} - \text{the correction factor for curvature of}$$

a cylindrical shell and for an increase in stress owing to radial strains in the vicinity of the crack tip. Functions M_F and p differ in form for the lowest point of the crack tip (point A in

Fig. 1) and for the crack mouth on the surface of the cylindrical shell (point B in Fig. 1).

C. Estimating the J integral – the FC method

This method was proposed in Addendum A16 of the French nuclear code RCC-MR [16]. It stems from the second option of describing the transition state between the ideally elastic behaviour and the fully plastic behaviour of a material, as suggested in the R6 method [17]. Considering the Ramberg-Osgood form of the stress-strain dependence (4) we can arrive at (5):

$$\frac{\varepsilon}{\varepsilon_0} = \frac{\sigma}{\sigma_0} + \alpha \left(\frac{\sigma}{\sigma_0} \right)^n \quad (4)$$

$$J = \frac{K^2}{E'} \left[A + \frac{0.5(\sigma/\sigma_0)^2}{A} \right] \quad (5)$$

where :

σ_0 is usually taken as the yield stress and $\varepsilon_0 = \sigma_0/E$

α, n are material constants

$E' = E$ for the plane stress

$E' = \frac{E}{1 - \nu^2}$ for the plane strain

ν is Poisson's ratio

$$A = 1 + \alpha \left(\frac{\sigma}{\sigma_0} \right)^n$$

The stress σ in the above equations is a nominal stress – i.e. a stress acting in the plane where the crack occurs. Referring to the R6 method [17] this stress may be written as:

$$\sigma = \frac{\sigma_\phi}{1 - \frac{\pi a c}{2t(t + 2c)}} \quad (6)$$

In (6) $\sigma_\phi = \frac{pD}{2t}$ is the hoop stress.

D. Estimating the J integral – the GS method

The GS method was derived on the basis of the limit transition of the J-integral, formally expressed for a semi-circular notch, to a crack, with the variation of the strain energy density along the notch circumference being approximated by the third power of the cosine function of the polar angle [18]. If under these assumptions, the stress-strain dependence is expressed by the Ramberg-Osgood relation (4) we can arrive at (7):

$$J = \frac{K^2}{E'} \left[1 + \frac{2\alpha n}{(n+1)} \left(\frac{\sigma}{\sigma_0} \right)^{n-1} \right] \quad (7)$$

where:

σ is the nominal stress given by (6).

III. TAKING INTO ACCOUNT THE CRACK TIP CONSTRAINT

The theory of single-parameter fracture mechanics assumes that the fracture toughness values obtained on laboratory specimens can be applied to a structural component. However, two-parameter approaches, such as the J-Q theory, reveal that the specimen must be tested under the same constraint as that of the body with a crack. In other words, the two geometries must have the same J-Q value at the moment of fracture so that the corresponding critical J-integral values, J_{cr} , will be equal to each other. Since J_{cr} values are often widely scattered, we cannot make a clear-cut prediction of this quantity. Only a certain range of plausible J_{cr} values can be predicted for a given body or structure. It should also be noted that the J-Q approach is only descriptive, and not predictive. This implies that the J-Q parameter quantifies the constraint at the crack tip without providing any indication of the particular influence of the constraint on the fracture toughness. Two-parameter theories cannot be strictly correct as far as their universality is concerned, because they assume two degrees of freedom. A study by Ainsworth and O'Dowd [19] on the influence of a constraint at the crack tip on fracture toughness indicates that geometries with a low constraint can in many cases be judged by a two-parameter theory, and geometries with a high constraint by a single-parameter theory.

A simple procedure based on the use of the so-called plastic constraint factor C has been applied in this paper to determine the fracture conditions in a thin-walled pressure pipeline. This factor is given by the ratio of the maximum principal stress to the HMM stress at the crack tip. When the HMM stress reaches the yield stress, the maximum principal stress obtains a value that is C times higher. This is in accordance with the observation that at a multi-axial state of stress the material behaves as if its yield stress were higher. This is to say that e.g. in the direction that the maximum stress acts, a stress higher than the yield stress should be applied to reach the beginning of plastic strains. Let us now consider the state of stress at the crack tip in a thick-walled body, where the stress perpendicular to the crack plane, σ_1 , and the stress in the direction of the crack, σ_2 , are equal, and the stress in the direction of the thickness of the body, σ_3 , is governed by the expression $\sigma_3 = \nu(\sigma_1 + \sigma_2)$. Then, based on the HMM criterion and the assumed elastic conditions $\nu \approx 0.33$, the plastic constraint factor $C \approx 3$. If the stress in the thickness direction, σ_3 , falls within $2\nu\sigma_1$ and zero (a thin-walled body), the value of the plastic constraint factor will range between $C = 1$ and $C = 3$. Let us now consider the state of stress at the crack tip of an external axial part-through crack in the wall of a test pipe

loaded by internal pressure. The thickness direction stress σ_2 is equal to the circumferential stress σ_1 , and the axial stress σ_3 is a fraction of the circumferential stress, i.e. $\sigma_3 = x\sigma_1$. Then the plastic constraint factor comes to $C = \frac{1}{1-x}$. This means

that in fracture analysis by (5) and (7) the value $C\sigma_0$ should be used instead of the uniaxial yield stress σ_0 . It was found that if the fraction $x = \sigma_3 / \sigma_1$ was taken to be 0.5 and subsequently the C factor to be 2, very good agreement was found between the predicted magnitude of the crack depth a_{cr} and the experimental magnitude for a particular axial crack in a DIA 1000/12 test pipe made of X70 steel.

It should be noted that the actual fracture toughness for the axial part-through crack geometry is greater than that obtained on CT specimens, because of a lower constraint; the real C factor is also lower, so that the J - a curve is steeper than that for a greater C factor. Due to this, the J integral for the axial part-through crack reaches the corresponding higher fracture toughness (for a lower constraint) for the same crack depth as the J integral with a higher C factor reaches lower fracture toughness (determined on CT specimens). The situation is illustrated in Fig.2.

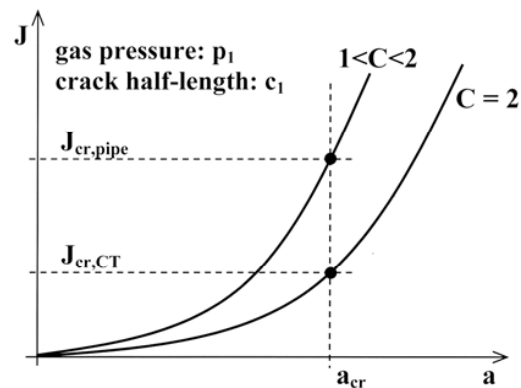


Fig. 2 Schematic representation of the J-a dependence for the constraint characteristic for (i) a CT specimen, and (ii) an axial part-through crack in a pipe

IV. BASIC MECHANICAL AND FRACTURE – MECHANICAL TESTS

The fracture condition of pressure pipelines was investigated on three test pipes with five cracks in the wall, the cracks being prepared by pressure cycling. The materials of the test pipes were X52, X65 and X70 steels.

The static tensile properties of these steels were obtained on flat specimens. They were taken in a circumferential direction of the pipes and were straightened afterwards. The stress-strain curves were analyzed and described by the Ramberg-Osgood dependence.

The fracture toughness of the materials of the pipe sections was determined using the J-based R curve, obtained on CT specimens with the starting notch being parallel with the axial direction of the pipe. The value of the J integral which corresponds to the attainment of maximum force at the “force-

force point displacement” curve was taken as the critical value, since it corresponds to the crack instability point for load-controlled loading of a body. The results of mechanical and fracture-mechanical tests are presented in Table I.

TABLE I
MECHANICAL AND FRACTURE-MECHANICAL PROPERTIES OF TESTED STEELS

Steel	X52	X65	X70
σ_y (MPa)	395	496	536
σ_{U} (MPa)	502	582	643
J_{cr} (N/mm)	415	432	439

σ_y : 0.2% proof stress; σ_U : ultimate tensile strength; J_{cr} : fracture toughness

V. TESTS ON THE TEST PIPES

A. Manufacture of the starting slits

In order to produce part-through cracks in the pipe wall, starting slits were manufactured on the surface of the pipe. They functioned as initiation notches for the development of cracks during subsequent cyclic pressurization of the test pipe. Starting slits can generally be made in several ways, one of which uses a thin grinding wheel. Such a grinding wheel was used in this study. The thickness of the wheel was 1.2 mm and the corresponding width of the slits made with it was approximately 1.5 mm. The starting slits were provided in the base material, the transition region and/or the weld metal, and their orientation was axial, circumferential or along the spiral weld.

The analysis showed that the physical depth of an initiated fatigue crack must be at least 0.5 mm along the whole perimeter of the slit tip so that the slit with the initiated crack at its tip can be considered as a crack after the test pipe has been subjected to cycling. This value follows from [20]. If such a crack a_t in size finds itself in a notch root defined by depth a_v and radius of roundness ρ (see Fig. 3), this configuration can be regarded as a surface crack a_e in depth, where

$$a_e = \left(1 + 7.69 \sqrt{\frac{a_v}{\rho}} \right) a_t \quad \dots\dots a_t < 0.13 \sqrt{a_v \rho} \quad (8)$$

$$a_e = a_v + a_t \quad \dots\dots a_t \geq 0.13 \sqrt{a_v \rho}$$

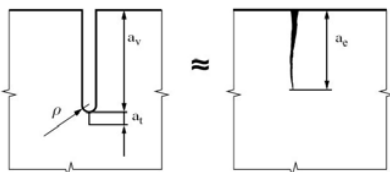


Fig. 3 Substitution of the notch with a crack by the equivalent crack

It is evident that for $a_t \geq 0.13 \sqrt{a_v \rho}$ a slit with a crack along the perimeter of the slit tip can be taken as a crack $a_v + a_t$ in depth. For slit width $2\rho = 1.5 - 2.0$ mm and notch depth $a_v = 6 - 10$ mm (in relation to wall thickness) we find

that the fatigue increment of the size of the initiated crack, a/t , should be greater than about 0.5 mm. In addition to working starting slits there were also manufactured so-called check slits, which were of the same surface length as the working slits but their depth was greater. These check slits functioned as a safety measure to prevent cracks that developed from the working slits penetrating through the pipe wall.

Three test pipes, made of X52, X65 and X70 steels, were provided with working slits and check slits. For illustration, a DN1000 test pipe is shown in Fig. 4.

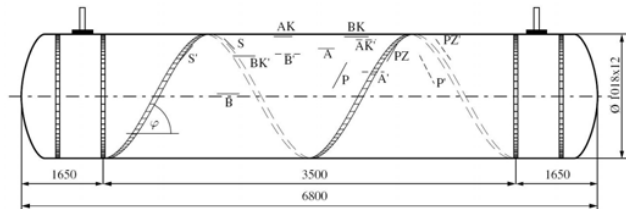


Fig. 4 Test pipe DN1000 with marking the starting slits

The outside diameter of this test pipe is $D = 1018$ mm, and the wall thickness is $t = 12$ mm. It is made of thermo-mechanically treated X70 steel according to API specification and is spirally welded, the weld being inclined at an angle of $\phi = 62^\circ$ to the pipe axis. It is provided with starting slits (see Table II for dimensions) oriented either axially or in the direction of the strip axis (i.e. in the direction of the spiral) and then along or inside the spiral weld. The slits differ in length ($2c=115$ mm or 230mm) and depth ($a=5, 6.5, 7,$ and 7.5mm).

TABLE II
DIMENSIONS OF THE STARTING SLITS

Defect - designation	Nominal dimensions		Actual dimensions	
	$2c(mm) \times a(mm)$		$2c(mm) \times a(mm)$	
A - base material	115	6.5	116	6.7
A' - base material	115	6.5	118	6.2
B - base material	230	5.0	232	5.3
B' - base material	230	5.0	255	4.9
AK - base material	115	7.5	117	8.0
AK' - base material	115	7.5	118	8.0
BK - base material	230	6.5	230	6.5
BK' - base material	230	6.5	228	6.7
P - base material	230	7.0	230	6.3
P' - base material	230	7.0	230	7.3
S - weld metal	230	5.0	230	5.0
S' - weld metal	230	5.0	230	6.0
PZ - transition region	230	5.0	230	4.6
PZ' - transition region	230	5.0	230	5.0

Efforts were made in the fracture tests to keep the circumferential fracture stress below the yield stress, because the operating stress in gas pipelines is virtually around one half of the yield stress (and does not exceed two thirds of the yield stress even in intrastate high-pressure gas transmission pipelines). Calculations reveal that in order to comply with this, the depth of the axial semi-elliptical cracks should be greater than one half of the wall thickness. Oblique cracks should be even deeper, as the normal stress component opening these cracks is smaller. If the crack depth is to have a

certain magnitude before the fracture test is begun, the depth of the starting slit should be smaller than this magnitude by the fatigue extension of the crack along the perimeter of the slit tip. At the same time, we should bear in mind that the higher the fatigue extension of the crack, the better the agreement with a real crack.

B. Cycling of cracks

After the starting slits were made, the test pipes were subjected to water pressure cycling to produce fatigue cracks in the tips of the starting slits. The cycling was carried out in a pressurizing system, which included a high-pressure water pump, a collecting tank, a regulator designed to control the amount of water that was supplied and, consequently, the rate at which the pressure is increased in the pipe section. This was effected by opening by-pass valves. A scheme of the pressurizing system is shown in Fig.5.

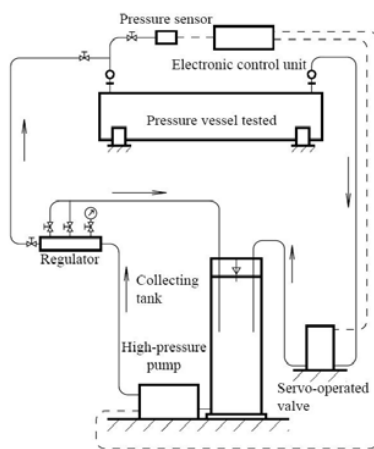


Fig. 5 Pressurizing system

In cycling the cracks, the water pressure fluctuated between $p_{\min} = 1.5$ MPa and $p_{\max} = 5.3$ MPa, and the number of pressure cycles was between 3 000 and 4 000. The period of a cycle was approximately 150 seconds.

The cycling went on until a crack initiated in one of the check slits became a through crack. This moment was easy to detect, because it was accompanied by a water leak. By choosing an appropriate difference between the depths of the working slits and the check slits it was possible to obtain a working crack depth (= starting slit depth + fatigue crack extension) approximately of the required size. To run a test for a fracture, however, it was necessary to remove the check slit which had penetrated through the wall of the test pipe from the body shell and to repair the shell, e.g. by welding a patch in it.

C. Fracture tests

After removing the check slit which penetrated through the wall, and repairing the shell of the test pipe, the pipe was loaded by increasing water pressure to burst. The test procedure, which was common to all test pipes, will now be

briefly described for the DN1000 pipe shown in Fig.3. As the figure suggests, slits A, A', B and B' were oriented along the axis of the pipe. Referring to Table II, we find that the nominal length of notches B, B' had twice the length of notches A, A', but that they were shallower.

As mentioned above, cracks at the slit tips were extended by fluctuating water pressure, and this proceeded until the cracks from the check slits (BK, BK') grew through the wall and a water leak developed. Then the damaged parts of the shell were cut out, patches were welded in their place, and the test pipe was monotonically loaded to fracture at the location of crack B or B'. The burst of the test pipe at crack B is shown in Figs. 6 and 7 (in detail).

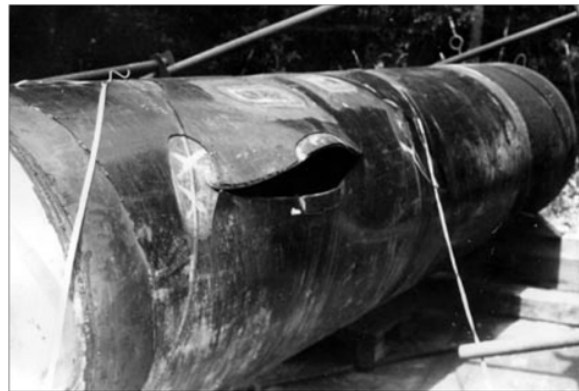


Fig. 6 Burst initiated on the slit B with a fatigue crack

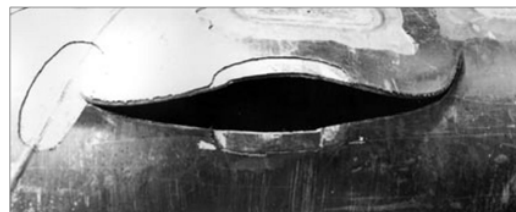


Fig. 7 Burst initiated on the slit B - detail

A part of the fracture surface is shown in Fig. 8.

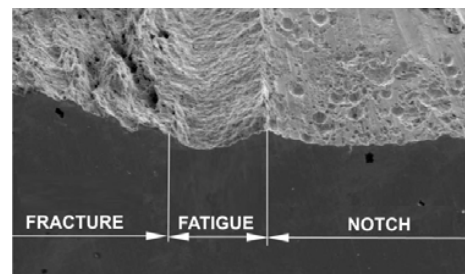


Fig. 8 A part of the fracture surface of the crack B

Evidently, at the instant of fracture the crack spread not only

through the remaining ligament, but also lengthwise. After removing the part of the pipe shell with crack B, a patch was welded in and the second burst test followed. Table III lists the numerical values of the geometrical parameters, the J-integral fracture values, the Ramberg-Osgood constants, the fracture pressure and the fracture depth for cracks B and B', respectively. Summary results are presented in Table IV. It should be noted that the tables include the Ramberg-Osgood constants for the circumferential direction of the test pipe, with the crack oriented axially in the pipe. This is because the stress-strain properties perpendicular to the crack plane are crucial in determining the J-integral for an axial crack. The stress-strain dependence in the circumferential direction should therefore be taken into account where an axial orientation of the crack is concerned.

The most important fracture test results from the viewpoint of fracture conditions are the magnitudes of the fracture pressure, p_f , and the fracture depth, a_f , for a given crack $2c$ in length. It follows from these tables that $p_f = 9.55$ MPa and $a_f = 7.1$ mm for crack B and $p_f = 9.86$ MPa and $a_f = 6.7$ mm for crack B'. These values are shown in the last two columns of Table IV.

Now let us predict the fracture conditions according to engineering approaches, and compare the prediction results with real fracture parameter values (pressure, crack depth). The procedure for verifying the engineering methods for predictions involves determining either the fracture stress for a given (fracture) crack depth or the fracture crack depth for a given (fracture) pressure.

TABLE III
FRACTURE PARAMETERS OF CRACK B AND B'

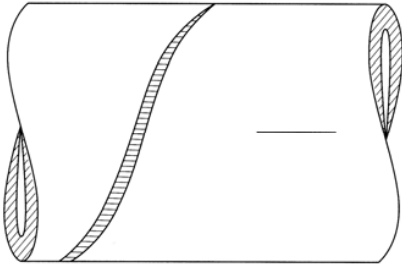
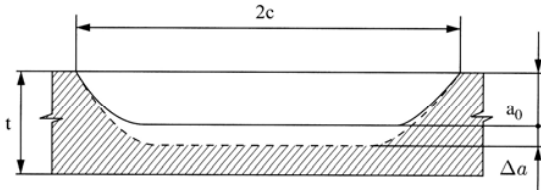
Dimensions: DIA 1018 x 12		Material: X70	
Location		Geometrical parameters	
			
CRACK – designation: B			
	t (mm)	c (mm)	a_0 (mm)
	11.7	115	4.7
FRACTURE VALUES OF J-INTEGRAL		J_{in} (N/mm)	J_{cr} (N/mm)
Longitudinal direction		357	439
RAMBERG-OSGOOD CHARACTERISTICS			
Characteristic		α	n
Circumferential direction		5.92	9.62
FRACTURE PRESSURE (MPa)			σ_0 (MPa)
Under monotonic load			536
FRACTURE DEPTH OF CRACK (mm)			7.1
CRACK – designation: B'			
	t (mm)	c (mm)	a_0 (mm)
	11.7	127	4.7
FRACTURE VALUES OF J-INTEGRAL		J_{in} (N/mm)	J_{cr} (N/mm)
Longitudinal direction		357	439
RAMBERG-OSGOOD CHARACTERISTICS			
Characteristic		α	n
Circumferential direction		5.92	9.62
FRACTURE PRESSURE (MPa)			σ_0 (MPa)
Under monotonic load			536
FRACTURE DEPTH OF CRACK (mm)			6.7

TABLE IV
SUMMARY OF DATA CONCERNING THE ASSESSMENT OF THE FRACTURE
BEHAVIOUR OF TEST PIPES

Material	X 52	X 65	X 65	X 70	X 70
D (mm)	820	820	820	1018	1018
t (mm)	10.2	10.7	10.6	11.7	11.7
c (mm)	50	100	100	127	115
a (mm)	7.0	7.7	7.0	6.7	7.1
a/t	0.686	0.720	0.660	0.573	0.607
a/c	0.14	0.077	0.07	0.053	0.062
p (MPa)	9.36	9.71	9.86	9.86	9.55
p/p _{0.2}	0.95	0.750	0.769	0.800	0.775
σ ₀ (MPa)	395	496	496	536	536
α	5.87	5.34	5.34	5.92	5.92
n	8.24	8.45	8.45	9.62	9.62
C	2.2	2.4	2.3	2.07	2.0
J _{cr} (N/mm)	415	432	432	439	439

To illustrate this, we select the latter case – i.e. determining the fracture depth of a crack for a given (fracture) pressure. Fig. 9 shows the J-integral vs. crack B depth dependences determined according to the FC and GS predictions for the fracture hoop stress given by the measured fracture pressure. In determining equations (5), (6), and (7), the following parameters were used for the calculation: $D = 1018$ mm; $t = 11.7$ mm; $p = p_f = 9.55$ MPa; $c = 115$ mm; $\alpha = 5.92$; $n = 9.62$; $\sigma_0 = 2 \times 536 = 1072$ MPa (i.e. $C = 2$).

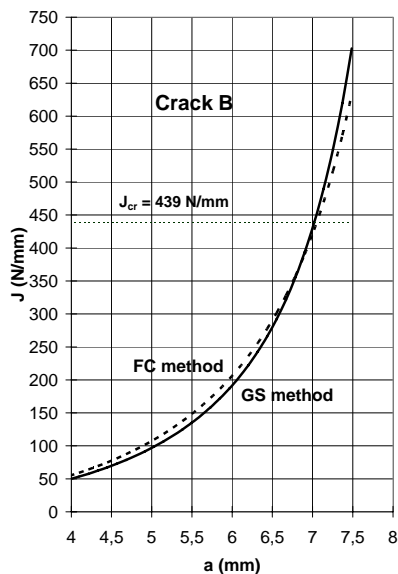


Fig. 9 Prediction of the fracture depth of the crack B for the pressure 9.55 MPa by the FC and GS methods

Fig. 10 shows similar dependences for crack B'. The same computational parameters as those employed in the case of crack B were used in the equations to determine the J-integral according to the FC and GS methods, with the exception of the fracture pressure ($p_f = 9.86$ MPa), the crack half-length ($c = 127$ mm) and C factor ($C = 2.07$).

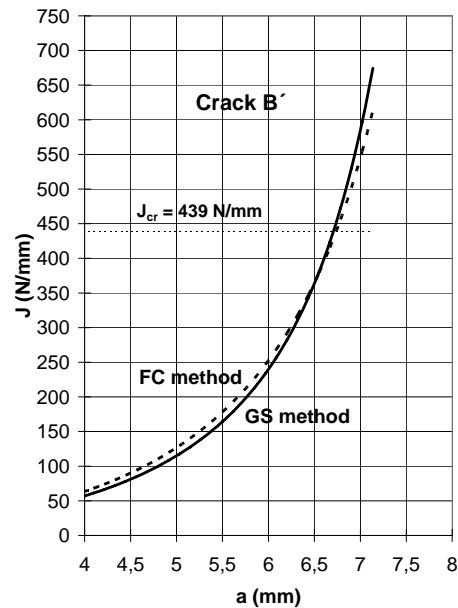


Fig. 10 Prediction of the fracture depth of the crack B' for the pressure 9.86 MPa by the FC and GS methods

As is evident from Fig. 9, the intersection of the straight line $J = J_{cr} = 439$ N/mm with the two $J - a$ curves gives the value $a_{cr} \approx 7.05$ mm, which is well consistent with the crack depth $B a_{cr} = 7.1$ mm established experimentally. Similarly, the intersection of the straight line $J = J_{cr} = 439$ N/mm with the $J - a$ curves according to the FC and GS procedures in Fig. 10 shows the fracture crack depth a_{cr} to be virtually identical to the experimentally found fracture depth $a_f = 6.7$ mm. For other test pipes, namely DIA 820/10.7, made of X65 steel and DIA 820/10.2 made of X52 steel, various magnitudes of the plastic constraint factor C were obtained to achieve good agreement of the geometric parameters at fracture with the experimental parameters. As expected, the magnitudes of the C factor depended on crack depth a_{cr} , as is illustrated in Fig. 11.

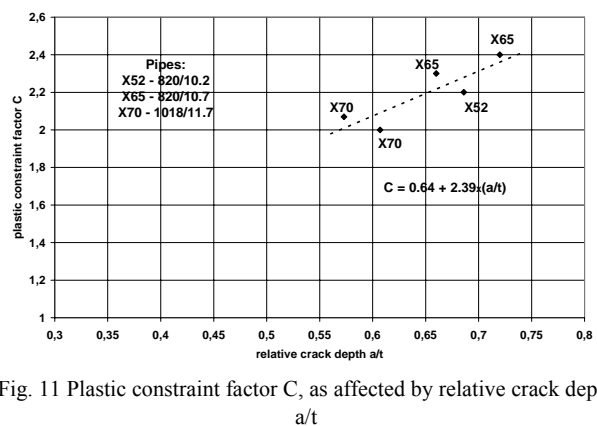


Fig. 11 Plastic constraint factor C, as affected by relative crack depth a/t

VI. CONCLUSIONS

On the basis of both experimental work and a fracture-mechanical evaluation of experimental results, an engineering method has been worked out for assessing the geometrical parameters of critical axial crack-like defects in a high-pressure gas pipeline wall for a given internal pressure of a gas. The method makes use of simple approximate expressions for determining fracture parameters K , J , and it accommodates the crack tip constraint effects by means of the so-called plastic constraint factor. Two independent approximate equations for determining the J -integral provided very close assessments of the critical geometrical dimensions of part-through axial cracks. With the use of our crack assessment method, the critical gas pressure in a pipeline can also be determined for a given crack geometry.

ACKNOWLEDGMENT

This work was supported by grant projects P105/10/2052 (GACR), P105/10/P555 (GACR), FT-TA5/076 (MPO), and by research plan AV0Z 20710524.

REFERENCES

- [1] S. Cravero and C. Ruggieri, "Structural Integrity Analysis of Axially Cracked Pipelines Using Conventional and Constraint - Modified Failure Assessment Diagrams," in *Int. Journal of Pressure Vessels and Piping* 83, 2006, pp. 607 – 617.
- [2] S. Saxena and D.S. Ramachandra Murthy, "Elastic - Plastic Fracture Mechanics Based Prediction of Crack Initiation Load in Through - Wall Cracked Pipes," in *Engineering Structures* 26, 2004, pp. 1165 - 1172.
- [3] J. Zemankova, "Instability of Surface Defects in a Thin-Walled Linepipe (in Czech)," in *Research Report V-KMtr-157/84*, CTU Prague, 1984
- [4] M.R. Ayatollahi and H. Khoramishad, "Stress Intensity Factors for an Axially Oriented Internal Crack Embedded in a Buried Pipe," in *Int. Journal of Pressure Vessels and Piping* 87, 2010, pp. 165 – 169
- [5] X. Wang and S.B. Lambert, "On the Calculation of Stress Intensity Factors for Surface Cracks in Welded Pipe-Plate and Tubular Joints," in *Int. Journal of Fatigue* 25, 2003, pp. 89 - 96
- [6] X. Wang and S.B. Lambert, "Stress Intensity Factors and Weight Functions for Longitudinal Semi-Elliptical Surface Cracks in Thin Pipes," in *Int. Journal of Pressure Vessels and Piping* 65, 1996, pp. 75 - 87
- [7] T.L. Anderson, *Fracture Mechanics: Fundamentals and Applications*. 3rd Edition. New York: CRC Press; 2005
- [8] C. Betegon and J.W. Hancock, "Two-Parameter Characterization of Elastic-Plastic Crack-Tip Fields," in *Journal of Applied Mechanics* 58, 1991, pp. 104 – 110
- [9] F. Wallner, F.M. Oberhauser, and H. Mildner, "Evaluation of the Behaviour of Large Pressure Vessels by Means of Fracture Mechanics Tests," in *International Conference: Fracture Toughness Testing – Methods, Interpretation and Application*, The Welding Institute, London 9-10 June 1982
- [10] S. Cravero and C. Ruggieri, "Correlation of Fracture Behavior in High Pressure Pipelines with Axial Flaws Using Constraint Designed Test Specimens - Part I: Plane – Strain Analyses," in *Engineering Fracture Mechanics* 72, 2005, pp. 1344 – 1360
- [11] I.S. Raju and J.C. Newman, Jr., "Stress Intensity Factors for Internal and External Surface Cracks in Cylindrical Vessels," in *Journal of Pressure Vessel Technology* 104, 1982, pp. 293 – 298
- [12] J.C. Newman and I.S. Raju, "An Empirical Stress Intensity Factor Equation for the Surface Crack," in *Engineering Fracture Mechanics* 15, 1981, pp. 185 – 192
- [13] Y. Murakami, *Stress Intensity Factors Handbook*. The Society of Materials Science, Japan, Pergamon Press, Oxford, 1987
- [14] E.S. Folias, "On the Theory of Fracture of Curved Sheets," in *Engineering Fracture Mechanics*, No.2, Vol.2, 1970, pp. 151-164
- [15] J.C. Newman, "Fracture Analysis of Surface and Through-Cracked Sheets and Plates," in *Engineering Fracture Mechanics*, Vol.5, No.3, 1973, pp. 667-689
- [16] RCC-MR: *Design and Construction Rules for Mechanical Components of FBR Nuclear Island*. First Edition (AFCEN - 3-5 Av. De Friedeland Paris 8), 1985
- [17] I. Milne, R.A. Ainsworth, A.R. Dowling, and A.T. Stewart, "Assessment of the Integrity of Structures Containing Defects," in *CEGB Report No. R/H/R6 - Rev.3*, Central Electricity Generating Board, London, United Kingdom, 1986.
- [18] L. Gajdoš and M. Srnc, "An Approximate Method for J Integral Determination," in *Acta Technica CSAV*, Vol.39, No.2, 1994, pp.151-171
- [19] R.A. Ainsworth and N.P. O'Dowd, "Constraint in the Failure Assessment Diagram Approach for Fracture Assessment, Trans. ASME," in *Journal of Pressure Vessel Technology*, Vol.117, 1995, pp. 260-267
- [20] R.A. Smith and K.J. Miller, "Fatigue Cracks at Notches," in *International Journal of Mechanical Sciences*, Vol.19, 1977, pp.11-22.